Physicochemical Characterization of σ-Bonded Aryl Iron(III) Porphycenes. X-ray Structures of (EtioPc)Fe(3,5-$C_6F_2H_3$) and (EtioPc)In(C_6H_5), Where EtioPc Is the Dianion of 2,7,12,17-Tetraethyl-3,6,13,16-tetramethylporphycene

Karl M. Kadish,*[,1a] Alain Tabard,[1b] Eric Van Caemelbecke,[1a] Ally M. Aukauloo,[1b] Philippe Richard,[1b] and Roger Guilard*[,1b]

Department of Chemistry, University of Houston, Houston, Texas 77204-5641, and LIMSAG, UMR 5633, Université de Bourgogne, Faculté des Sciences "Gabriel", 6 Boulevard Gabriel, 21100 Dijon, France

Received June 1, 1998

A series of iron(III) σ-bonded porphycenes are characterized by their electrochemical and spectroscopic properties. The investigated compounds are represented as (EtioPc)Fe(R), where EtioPc = the dianion of 2,7,12,17-tetraethyl-3,6,13,16-tetramethylporphycene and R = C_6H_5, 3,5-$C_6F_2H_3$, 3,4,5-$C_6F_3H_2$ or 2,3,5,6-C_6F_4H. Each compound is characterized as to its ESR, NMR, and UV−visible properties which are compared to corresponding compounds in an analogous series of (OEP)Fe(R) and (OETPP)Fe(R) derivatives where OEP and OETPP are the dianions of octaethyl- and octaethyltetraphenylporphyrin, respectively. The (EtioPc)Fe(R) complexes contain either high- or low-spin Fe(III), depending on the specific axial ligand and the temperature. The first oxidation of each (EtioPc)-Fe(R) complex involves a metal-centered reaction while the other electron transfers involve the addition or abstraction of electrons from the conjugated π-ring system of the porphycene. An X-ray crystal structure of low-spin (EtioPc)Fe(3,5-$C_6F_2H_3$) was obtained and compared to that of the analogous (EtioPc)In(C_6H_5). The iron etioporphycene crystallizes in the monoclinic system $P2_1/n$, and the iron atom lies close to the plane of the four porphycene nitrogen atoms ($\langle\Delta 4N-Fe\rangle = 0.12$ Å). The indium etioporphycene crystallizes in the monoclinic system $P2_1/n$, and the indium atom lies 0.85 Å above the plane of the four porphycene nitrogen atoms.

Introduction

A number of iron porphyrins with σ-bonded methyl, phenyl and substituted phenyl axial ligands have been synthesized and characterized as to their structural and physicochemical properties.[2−37] Previous studies of σ-bonded iron porphyrins have shown that the electronic configuration of the iron metal ion, i.e., the Fe(III) spin state, depends on several parameters,

(1) (a) University of Houston. (b) Université de Bourgogne.
(2) Cocolios, P.; Lagrange, G.; Guilard, R. *J. Organomet. Chem.* **1983**, *253*, 65−79.
(3) Mansuy, D. *Pure Appl. Chem.* **1980**, *52*, 681−690.
(4) Doppelt, P. *Inorg. Chem.* **1984**, *23*, 4009−4011.
(5) Lançon, D.; Cocolios, P.; Guilard, R.; Kadish, K. M. *J. Am. Chem. Soc.* **1984**, *106*, 4472−4478.
(6) Guilard, R.; Boisselier-Cocolios, B.; Tabard, A.; Cocolios, P.; Simonet, B.; Kadish, K. M. *Inorg. Chem.* **1985**, *24*, 2509−2520.
(7) Ortiz de Montellano, P. R.; Kerr, D. E. *Biochemistry* **1985**, *24*, 1147−1152.
(8) Balch, A. L.; Renner, M. W. *J. Am. Chem. Soc.* **1986**, *108*, 2603−2608.
(9) Balch, A. L.; Renner, M. W. *Inorg. Chem.* **1986**, *25*, 303−307.
(10) Brothers, P. J.; Collman, J. P. *Acc. Chem. Res.* **1986**, *19*, 209−215.
(11) Lexa, D.; Savéant, J.-M.; Wang, D. L. *Organometallics* **1986**, *5*, 1428−1434.
(12) Scheidt, W. R.; Chipman, D. M. *J. Am. Chem. Soc.* **1986**, *108*, 1163−1167.
(13) Arasasingham, R. D.; Balch, A. L.; Latos-Grazynski, L. *J. Am. Chem. Soc.* **1987**, *109*, 5846−5847.
(14) Battioni, J.-P.; Dupre, D.; Mansuy, D. *J. Organomet. Chem.* **1987**, *328*, 173−184.
(15) Brault, D.; Neta, P. *J. Phys. Chem.* **1987**, *91*, 4156−4160.
(16) Guilard, R.; Lecomte, C.; Kadish, K. M. *Struct. Bonding* **1987**, *64*, 205−268.
(17) Arafa, I. M.; Shin, K.; Goff, H. M. *J. Am. Chem. Soc.* **1988**, *110*, 5228−5229.
(18) Gueutin, C.; Lexa, D.; Savéant, J.-M. *Organometallics* **1989**, *8*, 1607−1613.
(19) Guilard, R.; Kadish, K. M. *Chem. Rev.* **1988**, *88*, 1121−1146.
(20) Guilard, R.; Mitaine, P.; Moïse, C.; Cocolios, P.; Kadish, K. M. *New J. Chem.* **1988**, *12*, 699−705.
(21) Kim, Y. O.; Goff, H. M. *J. Am. Chem. Soc.* **1988**, *110*, 8706−8707.
(22) Tabard, A.; Cocolios, P.; Lagrange, G.; Gerardin, R.; Hubsch, J.; Lecomte, C.; Zarembowitch, J.; Guilard, R. *Inorg. Chem.* **1988**, *27*, 110−117.
(23) Arasasingham, R. D.; Balch, A. L.; Hart, R. L.; Latos-Grazynski, L. *J. Am. Chem. Soc.* **1990**, *112*, 7566−7571.
(24) Gisselbrecht, J.-P.; Gross, M.; Köcher, M.; Lausmann, M.; Vogel, E. *J. Am. Chem. Soc.* **1990**, *112*, 8618−8620.
(25) Gueutin, C.; Lexa, D.; Momenteau, M.; Savéant, J.-M. *J. Am. Chem. Soc.* **1990**, *112*, 1874−1880.
(26) Shin, K.; Yu, B.-S.; Goff, H. M. *J. Am. Chem. Soc.* **1990**, *29*, 889−890.
(27) Guilard, R.; Perrot, I.; Tabard, A.; Richard, P.; Lecomte, C.; Liu, Y. H.; Kadish, K. M. *Inorg. Chem.* **1991**, *30*, 27−37.
(28) Kadish, K. M.; Tabard, A.; Lee, W.; Liu, Y. H.; Ratti, C.; Guilard, R. *Inorg. Chem.* **1991**, *30*, 1542−1549.
(29) Kano, K.; Takeuchi, M.; Hashimoto, S.; Yoshida, Z.-I. *J. Chem. Soc., Chem. Commun.* **1991**, 1728−1729.
(30) Swanson, B. A.; Dutton, D. R.; Lunetta, J. M.; Yang, C. S.; Ortiz de Montellano, P. R. *J. Biol. Chem.* **1991**, *266*, 19258−19264.
(31) Li, Z.; Goff, H. M. *Inorg. Chem.* **1992**, *31*, 1547−1548.
(32) Kadish, K. M.; D'Souza, F.; Van Caemelbecke, E.; Villard, A.; Lee, J.-D.; Tabard, A.; Guilard, R. *Inorg. Chem.* **1993**, *32*, 4179−4185.
(33) Kadish, K. M.; Boulas, P.; D'Souza, F.; Aukauloo, M. A.; Guilard, R.; Lausmann, M.; Vogel, E. *Inorg. Chem.* **1994**, *33*, 471−476.
(34) Kadish, K. M.; D'Souza, F.; Van Caemelbecke, E.; Boulas, P.; Vogel, E.; Aukauloo, A. M.; Guilard, R. *Inorg. Chem.* **1994**, *33*, 4474−4479.
(35) Kadish, K. M.; Van Caemelbecke, E.; D'Souza, F.; Medforth, C. J.; Smith, K. M.; Tabard, A.; Guilard, R. *Inorg. Chem.* **1995**, *34*, 2984−2989.
(36) Riordan, C. G.; Halpern, J. *Inorg. Chim. Acta* **1996**, *243*, 19−24.
(37) Kadish, K. M.; Van Caemelbecke, E.; Guiletii, E.; Fukuzumi, S.; Miyamoto, K.; Suenobu, T.; Tabard, A.; Guilard, R. *Inorg. Chem.* **1998**, *37*, 7, 1759−1766.

10.1021/ic980610o CCC: $15.00
Published on Web 10/29/1998

Chart 1

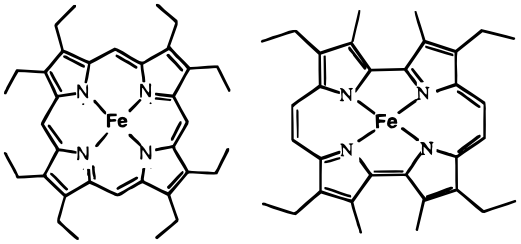

the most important of which are the nature of the macrocycle, the nature of the axial ligand, the solvent and the temperature.[22,28,37−39] In the OEP series (see Chart 1), the σ-bonded alkyl and phenyl complexes contain low-spin state iron(III) at room temperature. In contrast, OEP derivatives with an electron-withdrawing σ-bonded axial ligand such as 2,3,5,6-C_6F_4H or C_6F_5 are in a high-spin state, independent of the temperature.

Recently, it was shown that the two isomers of (OEP)Fe($C_6F_3H_2$), i.e., (OEP)Fe(3,4,5-$C_6F_3H_2$) and (OEP)Fe(2,4,6-$C_6F_3H_2$), which differ in the degree of steric hindrance between the axial ligand and the porphyrin macrocycle, are in different spin states.[37] The results of this study indicate that the nature of the axial ligand can have a strong effect on the chemical reactivity and spectroscopic properties of the σ-bonded iron porphyrins but less is known about the role of the macrocyclic ligand. Analogous σ-bonded aryl Fe(III) complexes in the oactethyltetraphenylporphyrin (OETPP) series contain a low-spin central metal ion, independent of the axial ligand or the temperature.[35] These results thus show that one cannot yet predict the behavior of all σ-bonded iron complexes with porphyrin or porphyrin-like macrocycles. It was therefore of interest to examine a new series of σ-bonded Fe(III) complexes containing a porphycene macrocycle which is one of the more recently studied isomers of the porphyrins.[40]

It now appears certain that (P)Fe(R) derivatives containing a porphyrin macrocycle such as OEP can be oxidized to Fe(IV) and reduced to Fe(II)[37] and a similar Fe(IV) oxidation state is seen for singly oxidized (EtioPc)Fe(C_6H_5) where EtioPc = the dianion of 2,7,12,17-tetraethyl-3,6,13,16-tetramethylporphycene (see Chart 1).[34]

In contrast, the reduction of (EtioPc)Fe(C_6H_5) does not lead to formation of Fe(II)[34] but rather gives an Fe(III) π anion radical and dianion, consistent with the lack of a metal-centered reduction in most transition-metal etioporphycenes.[41]

The present paper reports the synthesis and characterization of four new σ-bonded aryl iron(III) porphycenes which are represented as (EtioPc)Fe(R), where R = C_6H_5, 3,5-$C_6F_2H_3$, 3,4,5-$C_6F_3H_2$ or 2,3,5,6-C_6F_4H (Chart 2).

Each compound is characterized as to its ESR, NMR, UV−visible, and/or electrochemical properties and compared with a similar set of σ-bonded aryl iron(III) compounds containing an octaethylporphyrin macrocycle. We also present the X-ray crystal structure of (EtioPc)Fe(3,5-$C_6F_2H_3$) and an analogous σ-bonded phenyl complex containing a non-electroactive central metal ion, (EtioPc)In(C_6H_5).

Chart 2

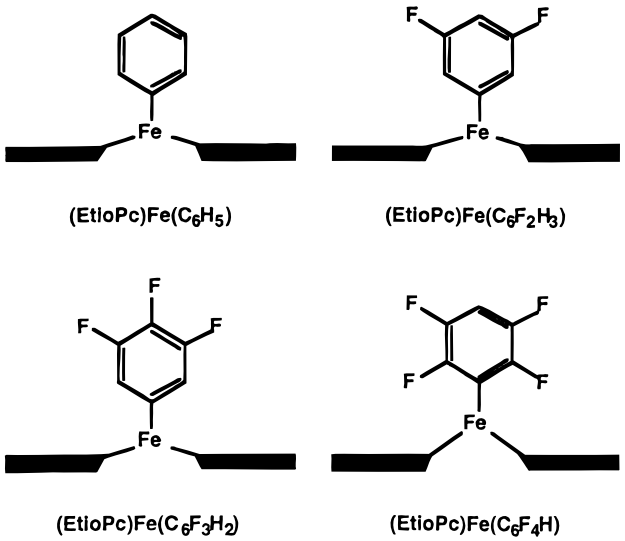

Experimental Section

Chemicals. Benzonitrile (PhCN) was obtained from Aldrich Chemical Co. and distilled over P_2O_5 under vacuum prior to use. Absolute dichloromethane (CH_2Cl_2) over molecular sieves (Fluka Chemika) and anhydrous pyridine (Aldrich) were used without further purification. Tetra-*n*-butylammonium perchlorate (TBAP) was purchased from Sigma Chemical Co., recrystallized from ethyl alcohol, and dried under vacuum at 40 °C for at least 1 week prior to use.

Synthesis. The synthesis of each porphycene was performed under an argon atmosphere. Schlenk techniques were used for all operations. Samples of (EtioPc)FeCl and (EtioPc)InCl were prepared as described in the literature[33,34] and were obtained by metalation of (EtioPc)H_2 with $FeCl_2$ or $InCl_3$. (EtioPc)In(C_6H_5) was prepared as reported in the literature.[34]

(EtioPc)Fe(R). Four different aryl σ-bonded iron porphycenes were prepared by reacting an aryl Grignard reagent with (EtioPc)FeCl according to literature procedures.[34] (EtioPc)Fe(C_6H_5) was prepared as reported in the literature.[34] (EtioPc)Fe(R), where R = 3,5-$C_6F_2H_3$, 3,4,5-$C_6F_3H_2$, or 2,3,5,6-C_6F_4H, have not previously been reported. Their synthesis proceeds as described for (EtioPc)Fe(C_6H_5),[34] and a description of their physicochemical properties is given below.

(EtioPc)Fe(3,5-$C_6F_2H_3$). MS (DCI), *m/z* (rel intensity): $M^{\bullet+}$ 645 (15); $[M - C_6F_2H_3]^+$ 532 (100). Elem. anal. calcd for $C_{38}H_{39}N_4F_2Fe$: C, 70.7; H, 6.1; N, 8.7. Found: C, 70.5; H, 6.5; N, 8.7.

(EtioPc)Fe(3,4,5-$C_6F_3H_2$). MS (DCI), *m/z* (rel intensity): $M^{\bullet+}$ 663 (14); $[M - C_6F_3H_2]^+$ 532 (100). Elem. anal. calcd for $C_{38}H_{38}N_4F_3Fe$: C, 68.7; H, 5.8; N, 8.4. Found: C, 68.8; H, 6.0; N, 8.5.

(EtioPc)Fe(2,3,5,6-C_6F_4H). MS (DCI), *m/z* (rel intensity): $M^{\bullet+}$ 681 (10); $[M - C_6F_4H]^+$ 532 (100). Elem. anal. calcd for $C_{38}H_{37}N_4F_4Fe$: C, 67.0; H, 5.5; N, 8.2. Found: C, 67.3; H, 5.4; N, 8.3.

Instrumentation. ^1H and ^{19}F NMR spectra were recorded at 500 MHz on a Bruker Avance DRX spectrometer at the CSMUB (Centre de Spectrométrie Moléculaire de l'Université de Bourgogne). ESR spectra were recorded in toluene on a Bruker ESP 300 spectrometer equipped with an Oxford Instrument Cryostat. The *g* values were measured with respect to diphenylpicrylhydrazyl ($g = 2.0036 \pm 0.0003$). UV−visible spectra were recorded on a Varian Cary 5 E spectrophotometer. Mass spectra in DCI or SIM/FD mode were obtained with a Kratos Concept 32S spectrometer and the data were collected and processed using a Sun 3/80 workstation. Cyclic voltammograms were obtained with an EG&G Princeton Applied Research

(38) Kadish, K. M.; D'Souza, F.; Van Caemelbecke, E.; Tabard, A.; Guilard, R. In *Proceedings of the Fifth International Symposium on Redox Mechanisms and Interfacial Properties of Molecules of Biological Importance*; Shultz, F. A., Taniguchi, I., Eds.; The Electrochemical Society, Inc.: Princeton, NJ, 1993; Vol. 93-II, pp 125−134.
(39) Kadish, K. M.; Van Caemelbecke, E.; D'Souza, F.; Medforth, C. J.; Smith, K. M.; Tabard, A.; Guilard, R. *Organometallics* **1993**, *12*, 2411−2413.
(40) Vogel, E.; Bröring, M.; Weghorn, S. J.; Scholz, P.; Deponte, R.; Lex, J.; Schmickler, H.; Schaffner, K.; Braslavsky, S. E.; Müller, M.; Pörting, S.; Fowler, C. J.; Sessler, J. L. *Angew. Chem., Int. Ed. Engl.* **1997**, *36*, 1651−1654.
(41) D'Souza, F.; Boulas, P.; Aukauloo, A. M.; Guilard, R.; Kisters, M.; Vogel, E.; Kadish, K. M. *J. Phys. Chem.* **1994**, *98*, 11885−11891.

Table 1. Crystal Data and Data Collection for (EtioPc)In(C_6H_5) and (EtioPc)Fe($C_6F_2H_3$)

	(EtioPc)In(C_6H_5)	(EtioPc)Fe($C_6F_2H_3$)
molecular formula	$C_{38}H_{41}InN_4$	$C_{38}H_{39}F_2FeN_4$
M_r	668.57	645.58
data collcn temp (K)	293(2)	293(2)
graphite-monochromated radiation (Å)	Mo Kα (λ = 0.710 73 Å)	Mo Kα (λ = 0.710 73 Å)
crystal system, space group	monoclinic, $P2_1/n$	monoclinic, $P2_1/n$
a (Å)	15.814(2)	13.579(3)
b (Å)	13.026(3)	16.070(3)
c (Å)	17.048(3)	14.516(3)
β (deg.)	112.89(1)	101.370(16)
V (Å^3)	3235.4(10)	3105.4(11)
Z, D_{calc} (g cm^{-3})	4, 1.373	4, 1.381
μ (mm^{-1})	0.763	0.532
F(000)	1384	1356
cryst size (mm^3)	3.2 × 2.5 × 2.0	1.8 × 1.5 × 1.0
$(\sin\theta/\lambda)_{max}$ (Å^{-1})	0.595	0.594
index ranges	$-18 \le h \le 17$	$-15 \le h \le 15$
	$0 \le k \le 15$	$-19 < k \le 0$
	$0 \le l \le 20$	$0 \le l \le 17$
no. of reflcns collcd/unique	5892/5689	5626/5405
no. of reflcns with $I > 3\sigma(I)$	4803	2772
R(int)	0.0214	0.0616
abs corr	none	none
decay (%)	0	4
refinement method	full-matrix least-squares on F^2	full-matrix least-squares on F^2
no. of data/restraints/params	5689/0/392	5405/0/410
goodness-of-fit on F^2	1.071	1.028
final R indices [$I > 2\sigma(I)$]	R1 = 0.0307	R1 = 0.0490
R indices (all data)[a]	R1 = 0.0411, wR2 = 0.0856	R1 = 0.1577, wR2 = 0.1479
largest diff peak and hole	0.978 and −0.770 e Å^{-3}	0.370 and −0.344 e Å^{-3}

[a] Weight = $1/[\sigma^2(F_o^2) + (0.0487P)^2 + 1.94P]$ for (EtioPc)In(C_6H_5) and weight = $1/[\sigma^2(F_o^2) + (0.0640P)^2 + 0.95P]$ for (EtioPc)Fe($C_6F_2H_3$), where $P = (\mathrm{Max}(F_o^2,0) + 2F_c^2)/3$.

model 173 potentiostat/galvanostat coupled with an EG&G PARC model 175 Universal Programmer. Current−voltage curves were recorded on a EG&G Princeton Applied Research model RE-0151 X-Y recorder. A three-electrode system was used and consisted of a glassy carbon button or platinum working electrode, a platinum wire counter electrode and a saturated calomel reference electrode (SCE). The reference electrode, was separated from the bulk of the solution by a fritted-glass bridge filled with the solvent/supporting electrolyte mixture. All potentials are referenced to the SCE.

Crystal and Molecular Structure Determination. Suitable crystals of (EtioPc)Fe($C_6F_2H_3$) and (EtioPc)In(C_6H_5) were mounted on a CAD4 Enraf Nonius diffractometer. Both compounds crystallize in the monoclinic system, space group $P2_1/n$. Experimental details are given in Table 1. A total of 5689 unique reflections were collected for (EtioPc)In(C_6H_5) (4803 with $I > 2\sigma(I)$), and 5405 were collected for (EtioPc)Fe($C_6F_2H_3$) (2772 with $I > 2\sigma(I)$). The structures were solved by interpretation of Patterson maps (SHELXS)[42] and refined anisotropically by standard full-matrix least-squares techniques (SHELXL).[43] Hydrogen atoms were included in calculated positions and allowed to ride on the carbon atoms. Final agreement indices for both compounds are reported in Table 1, while main bond distances and angles are listed in Table 2. Positional parameters, full bond distances and angles, anisotropic thermal parameters, and hydrogen coordinates are reported as Supporting Information.

Results and Discussion

Characterization of Neutral (EtioPc)Fe(R). Mass Spectrometry. Mass spectral data are given in the Experimental Section for each investigated compound. The fragmentation pattern is typical for organoiron tetrapyrrole complexes. A molecular peak is observed for each (EtioPc)Fe(R) derivative, and the parent peak corresponds to a species which has lost the σ-bonded axial ligand, the highest intensity being observed for R = C_6H_5 and the lowest for R = C_6F_4H. This result indicates that the covalent character of the metal−axial ligand bond decreases upon going from (EtioPc)Fe(C_6H_5) to (EtioPc)Fe(C_6F_4H) and this is consistent with the electron-withdrawing properties of the axial ligand. The mass spectra are in good agreement with the expected molecular formula of (EtioPc)Fe(R), with definitive proof for this assignment being given by comparison of the experimental and calculated mass spectral data.

Table 2. Selected Bond Lengths (Å) and Angles (deg) for (EtioPc)In(C_6H_5) and (EtioPc)Fe($C_6F_2H_3$)

	(EtioPc)Fe($C_6F_2H_3$)	(EtioPc)In(C_6H_5)
	Bond Distances (Å)	
M−N(1)	1.924(3)	2.170(2)
M−N(2)	1.928(3)	2.177(2)
M−N(3)	1.935(3)	2.174(2)
M−N(4)	1.931(3)	2.177(2)
M−C(33)	1.950(4)	2.148(3)
	Bond Angles (deg)	
N(1)−M−N(2)	81.61(14)	88.33(9)
N(1)−M−N(3)	171.96(14)	134.98(9)
N(1)−M−N(4)	97.97(15)	74.53(9)
N(2)−M−N(3)	97.90(15)	74.52(9)
N(2)−M−N(4)	173.40(14)	134.59(9)
N(3)−M−N(4)	81.58(15)	88.38(8)
N(1)−M−C(33)	93.22(17)	112.3(1)
N(2)−M−C(33)	95.30(15)	113.29(9)
N(3)−M−C(33)	94.82(16)	112.7(1)
N(4)−M−C(33)	91.30(16)	112.11(9)

NMR Spectroscopy. The ^{1}H NMR data of each (EtioPc)Fe(R) derivative are summarized in Table 3 and examples of the spectra for (EtioPc)FeCl and (EtioPc)Fe(C_6H_5) are shown in Figure 1. The data indicate that each compound is paramagnetic, but chemical shifts for the ethyl and methyl groups

(42) Sheldrick, G. M. *SHELXS-93: Program for Crystal Structure Determinations*; University of Göttingen: Göttingen, Federal Republic of Germany, 1993.
(43) Sheldrick, G. M. *SHELXL-97: Program for Crystal Structure Refinement*; University of Göttingen: Göttingen, Federal Republic of Germany, 1997.

Table 3. ^{1}H NMR (δ, ppm) Data for Investigated Complexes in $CDCl_3$ at 298 K with Isotropic Chemical Shifts ($(\Delta H/H)^{Iso}$) Given in Parentheses

	porphycene macrocycle					axial ligand		
compound	H 9,10,19,20	α-CH_2 2,7,12,17	α′-CH_2 2,7,12,17	α-CH_3 3,6,13,16	β-CH_3 2,7,12,17	*o*-H	*m*-H	*p*-H
(EtioPc)Fe(C_6H_5)	6.68	7.83	3.14	11.45	1.25	−5.46	3.49	−5.46
	(−3.10)	(4.04)	(−0.61)	(8.07)	(−0.42)	(−9.13)	(−2.12)	(−11.29)
(EtioPc)Fe($C_6F_2H_3$)	6.16	8.62	3.51	11.94	1.25	5.49		4.67
(EtioPc)Fe($C_6F_3H_2$)	5.96	8.69	3.58	11.91	1.25	6.12		
(EtioPc)Fe(C_6F_4H)	−14.14	34.04	32.76	75.70	6.98			1.27
(EtioPc)FeCl	−12.14	36.90	24.50	79.00	6.56			
	H 5,10,15,20	α-CH_2	α′-CH_2	β-CH_3				
(OEP)Fe(C_6H_5)[a]	5.53	4.46	−1.70	−1.76	−79.90	13.23		−23.80
	(−4.66)	(0.32)	(−5.84)	(−3.68)	(−82.61)	(−7.72)		(−29.64)

[a] Data from ref 2.

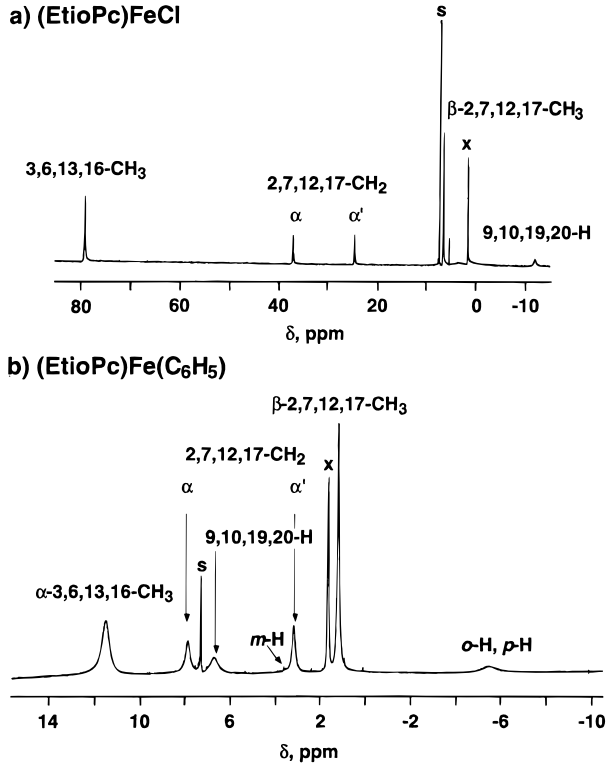

Figure 1. H NMR spectra of (a) (EtioPc)FeCl and (b) (EtioPc)Fe(C_6H_5) in $CDCl_3$ at 298 K (unknown impurity and solvent labeled as x and s).

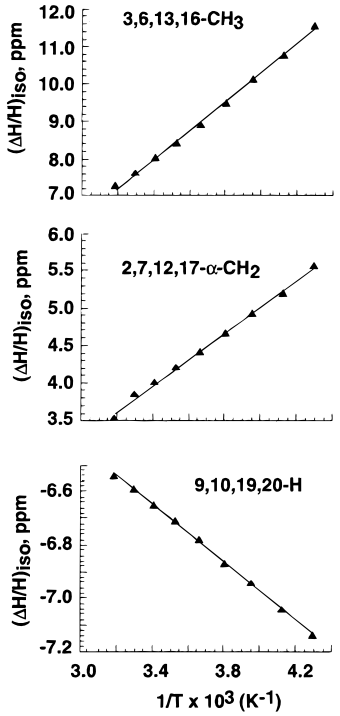

Figure 2. Curie plot of (EtioPc)Fe(C_6H_5) in $CDCl_3$.

of (EtioPc)Fe(C_6F_4H) and (EtioPc)FeCl are located at much lower field than signals for the same two proton groups of the other three investigated complexes, i.e., (EtioPc)Fe(C_6H_5), (EtioPc)Fe($C_6F_2H_3$), and (EtioPc)Fe($C_6F_3H_2$). Different NMR spectra are expected for the chloro and phenyl derivatives since these two porphycenes have different iron(III) spin states, i.e., low spin for (EtioPc)Fe(C_6H_5) and high spin for (EtioPc)FeCl.[34] This is indeed the case as shown in Figure 1 and Table 3. (EtioPc)Fe($C_6F_2H_3$) and (EtioPc)Fe($C_6F_3H_2$) contain low-spin iron(III) while (EtioPc)Fe(C_6F_4H) contains high-spin iron(III). A change in iron spin state occurs upon going from (OEP)Fe(C_6H_5) to (OEP)Fe(C_6F_4H) and this difference in spin state was explained on the basis of the stronger electron-withdrawing properties of the C_6F_4H group as compared to C_6H_5.[6]

A plot of the isotropic chemical shifts vs T^{-1} is shown in Figure 2 for the porphycene protons of (EtioPc)Fe(C_6H_5) in $CDCl_3$. The Curie plots show that $(\Delta H/H)_{iso}$ varies linearly with $1/T$ between 225 and 325 K and this agrees with the presence of low-spin iron(III) in the compound.[44] The isotropic chemical shifts of (EtioPc)Fe(C_6H_5) (Table 3) cover a smaller range than those for the previously studied (OEP)Fe(C_6H_5) derivative. This result thus indicates a lower iron electron-phenyl proton interaction in the EtioPc derivative. However, the absolute value of the *m*-H isotropic chemical shift is lower than values of *o*- and *p*-H for the two types of compounds, i.e., (OEP)Fe(C_6H_5) and (EtioPc)Fe(C_6H_5), and this was explained in the case of the OEP derivative on the basis of unpaired π-spin density on the σ-bonded phenyl group.[6] The NMR data in Table 3 also suggest the presence of unpaired π-spin density on the axial σ-bonded phenyl ligand, but the extent of delocalization is significantly smaller than in the case of the porphyrin analogue. Further evidence for spin delocalization is given by comparing *p*-H resonances of the C_6F_4H groups which are located at 1.27 ppm for (EtioPc)Fe(C_6F_4H) in $CDCl_3$ at 298 K and at −58.85 ppm for (OEP)Fe(C_6F_4H) in C_6D_6 at 294 K.[6] The iron porphycenes might have a coordination polyhedron geometry that does not favor a large iron−aryl orbital overlap. The X-ray crystal structure of (EtioPc)Fe($C_6F_2H_3$) has been solved and shows a quite different geometry as compared with

(44) La Mar, G. N.; Walker, F. A. In *The Porphyrins*; Dolphin, D., Ed.; Academic Press: New York, 1978; Vol. IV, pp 61−157.

Table 4. ESR Data of Investigated Low-Spin ($S = {}^1/_2$) Compounds in a 1:1 Toluene/CH_2Cl_2 Mixture at 100 K

compounds	g_x	g_y	g_z	Δ/λ	V/λ	V/Δ
(EtioPc)Fe(C_6H_5)	1.94	2.27	2.29	3.91	6.91	1.77
(EtioPc)Fe($C_6F_2H_3$)	1.93	2.26	2.29	4.01	6.70	1.67
(EtioPc)Fe($C_6F_3H_2$)	1.93	2.26	2.29	4.01	6.70	1.67
(EtioPc)Fe(C_6F_4H)	1.92	2.28	2.34	3.99	6.70	1.46

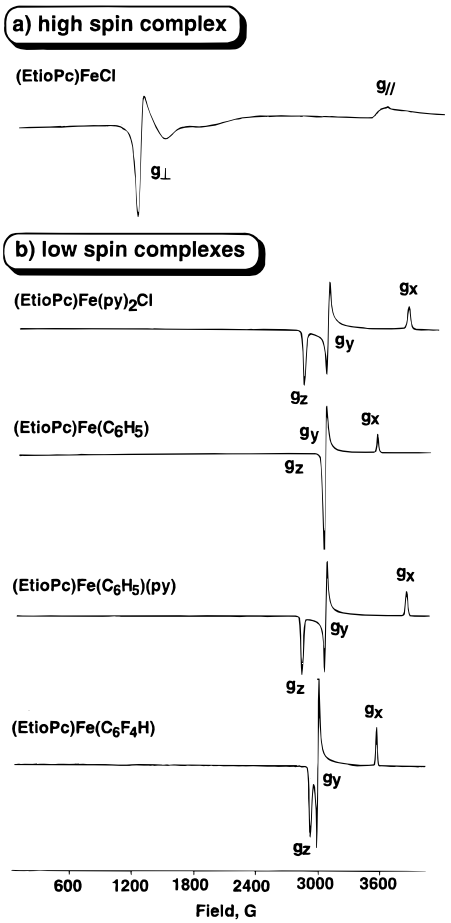

Figure 3. ESR spectra at 100 K of (a) high-spin and (b) low-spin Fe(III) complexes in 1:2 toluene/CH_2Cl_2 or 1:1:1 toluene/CH_2Cl_2/pyridine mixture for the case of $[(EtioPc)Fe(py)]_2^+Cl^-$ and (EtioPc)-Fe(C_6H_5)(py).

that of iron porphyrin complexes. This is described in the following section of the manuscript.

ESR Spectroscopy. The porphycene NMR data indicate that the nature of the axial ligand also influences, to a large extent, the spin state of the iron center. The C_6H_5, $C_6F_2H_3$ and $C_6F_3H_2$ derivatives all show NMR spectra which are characteristic of low spin iron(III) complexes while the NMR spectrum of (EtioPc)Fe(C_6F_4H) resembles that of a typical high-spin Fe(III) complex such as (EtioPc)FeCl. Surprisingly, the ESR data shows unexpected results for some of the same σ-bonded porphycene derivatives. The overall ESR data are summarized in Table 4 and examples of ESR spectra are shown in Figure 3. The spectrum of (EtioPc)FeCl is typical of a high-spin iron(III) complex in that it shows signals at $g = 2.00$ and 6.00 (see Figure 3a). The ESR data for (EtioPc)FeCl at 100 K are consistent with the NMR data at room temperature and this is also the case for the C_6H_5, $C_6F_2H_3$, and $C_6F_3H_2$ derivatives which, at 100 K, are all indicative of species containing low spin iron(III) (Table 4, Figure 3b). The g values range from 1.93 to 2.29 and are almost identical for all of the investigated porphycenes. The results for (EtioPc)Fe(C_6F_4H) contrast with those of the analogous (OEP)Fe(C_6F_4H) complex which contains high-spin Fe(III) independent of the temperature,[22] thus indicating that the local symmetry of the iron center is lower for compounds in the porphycene series than for those in the porphyrin series. This result might be explained by the fact that the porphycenes have a rectangular cavity[45,46] as compared to a quasi-square cavity in the case of porphyrins.[47] The rhombicity (V/Δ) and the tetragonal distortion (Δ/λ) of the low-spin porphycenes were calculated on the basis of the g values and these data are given in Table 4. Theoretical studies on iron porphyrins show that the limit of V/Δ is close to 0.66 for compounds having the largest rhombicity, i.e., the energy differences between the d_{xz}, d_{xy}, and d_{yz} orbitals are similar in a proper axis system.[48] The V/Δ values calculated for the porphycenes range from 1.46 to 1.77 (see Table 4). These simple calculations clearly indicate that the coordinate system used in the porphyrin series cannot be selected for the porphycene complexes. New theoretical studies are now in progress and should indicate if the electron configuration for the porphycenes and porphyrins are totally different.

The ESR data also point out an interesting behavior for (EtioPc)Fe(C_6F_4H). The ESR spectrum of this compound (Figure 3b) is typical of a complex containing a low spin iron(III) at 100 K while a high-spin electronic configuration is suggested by the NMR results at room temperature (see Table 3). The g_z value of 2.34 for (EtioPc)Fe(C_6F_4H) at 100 K is also higher than the g_z values for the other σ-bonded iron(III) porphycenes suggesting that (EtioPc)Fe(C_6F_4H) possesses the highest axial character among the investigated σ-bonded porphycene complex series. No spin transition has been observed by NMR spectroscopy in liquid solution over a range of temperature between 100 and 300 K. The change in the iron(III) spin state for (EtioPc)Fe(C_6F_4H) could have several origins,[22] but is most likely due to an effect of the solvent matrix upon going from liquid to a glass state as was earlier reported for several σ-bonded iron(III) porphyrins.[19] The electronic properties of (EtioPc)Fe(C_6F_4H) differ from those of (OEP)Fe(C_6F_4H) in that the electron-withdrawing character of the C_6F_4H axial ligand does not bring about a change from low spin to high spin as in the case of (EtioPc)Fe(C_6F_4H). A similar behavior is observed for (OETPP)Fe(R) whose derivatives synthesized to date all contain low-spin iron(III), independent of the temperature or the specific σ-bonded axial ligand.[35]

Six-coordinate (EtioPc)Fe(C_6H_5)(py) and $[(EtioPc)Fe(py)_2]^+Cl^-$ are formed from (EtioPc)Fe(R) and (EtioPc)FeCl in the presence of pyridine, and this is confirmed by the ESR spectra (Figure 3). The binding of a sixth axial ligand to low-spin (EtioPc)-Fe(C_6H_5) induces a large splitting of the ESR signals, and this is as expected when there is a change in iron coordination.[28]

UV−Visible Spectroscopy. The UV−visible spectral data of (EtioPc)FeCl and (EtioPc)Fe(R) are summarized in Table 5, and spectra of (EtioPc)Fe(C_6F_4H) and (EtioPc)Fe(C_6H_5) in CH_2Cl_2 are shown in Figure 4. (EtioPc)FeCl exhibits two main bands at 368 and 617 nm. The Soret band of (EtioPc)Fe(C_6F_4H) is red-shifted by 10 nm with respect to that of (EtioPc)FeCl. A larger red shift ($\approx$15 nm) is observed when the Soret band of (EtioPc)FeCl is compared to that of the three investigated low-spin (EtioPc)Fe(R) derivatives. Furthermore, each low-spin

(45) Vogel, E.; Köcher, M.; Schmickler, H.; Lex, J. *Angew. Chem., Int. Ed. Engl.* **1986**, *25*, 257−259.
(46) Sessler, J. L.; Weghorn, S. J. *Expanded, Contracted, and Isomeric Porphyrins*, 1st ed.; Elsevier Science Ltd: New York, 1997; p 520.
(47) Scheidt, W. R.; Lee, Y. J. *Struct. Bonding* **1987**, *64*, 1−70.
(48) Palmer, G. in *Iron Porphyrins*; Lever, A. B. P., Gray, H. B., Eds.; Addison-Wesley: Reading, MA, 1983; Vol. II, pp 43−88.

Table 5. UV−Visible Data (λ_{max}, nm ($\epsilon \times 10^{-3}$, M^{-1} cm^{-1})) in CH_2Cl_2 at Room Temperature (Band Notations Are Indicated in Figure 4)

		Soret region			visible bands		ratio
compound	spin state	I″	I′	I	α	β	ϵ(I)/ϵ(β)
(EtioPc)Fe(C_6H_5)	1/2	320 (40.5)	355 (66.9)	382 (65.0)	555 (17.5)	590 (44.4)	1.46
(EtioPc)Fe($C_6F_2H_3$)	1/2	320 (39.4)	360 (61.2)	383 (68.1)	560 (16.7)	593 (41.7)	1.63
(EtioPc)Fe($C_6F_3H_2$)	1/2	319 (38.7)	357 (60.1)	383 (68.2)	560 (16.5)	594 (40.9)	1.66
(EtioPc)Fe(C_6F_4H)	5/2	–	–	378 (78.7)	584 (10.5)	623 (35.1)	2.24
(EtioPc)FeCl	5/2	–	–	368 (88.2)	–	617 (36.5)	2.38

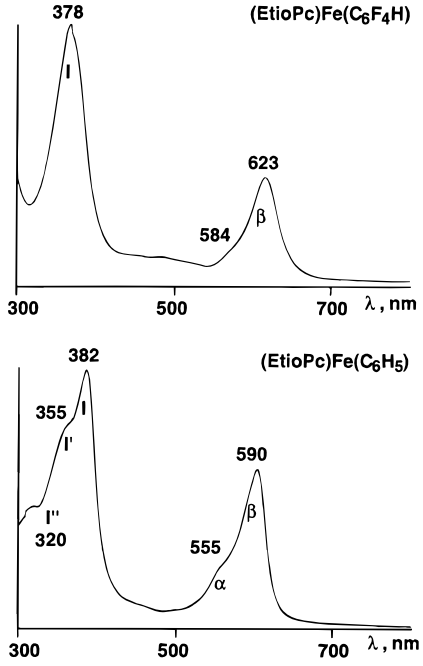

Figure 4. UV−visible spectra of (EtioPc)Fe(C_6F_4H) and (EtioPc)Fe(C_6H_5) in CH_2Cl_2.

σ-bonded iron(III) porphycene exhibits two additional bands in the near-UV region (bands I′ and I″ in Table 5). The Soret band of (EtioPc)Fe(C_6F_4H) is located at 378 nm and is blue-shifted by 4 nm with respect to the Soret band of (EtioPc)Fe(C_6H_5). The visible bands of (EtioPc)Fe(C_6F_4H) are red-shifted by 29 nm (band α) and 33 nm (band β) with respect to the corresponding visible bands of (EtioPc)Fe(C_6H_5). (EtioPc)Fe(C_6F_4H) shows only a single Soret band and lacks bands I′ and I″.

The UV−visible spectrum of (EtioPc)Fe(C_6F_4H) resembles the spectrum of (EtioPc)FeCl and both spectra differ significantly from spectra of the other investigated σ-bonded iron(III) porphycenes. The UV−visible data are consistent with the NMR results at room temperature in that both sets of spectral data indicate that (EtioPc)Fe(C_6F_4H) and (EtioPc)FeCl contain high-spin iron(III) at room temperature while the other σ-bonded iron(III) complexes contain low-spin iron(III) under the same experimental conditions. Further indirect evidence for these assignments is given by the ratio between band I and band β in the Soret and visible regions (see Table 5). The three low-spin complexes have a similar ratio of 1.46 to 1.66, while the two high-spin derivatives have ratios of 2.24 and 2.38. This result therefore indicates that the Fe−C bond of (EtioPc)Fe(C_6F_4H) has more ionic than covalent character.[49]

X-ray Structures of (EtioPc)In(C_6H_5) and (EtioPc)Fe(3,5-$C_6F_2H_3$). The (EtioPc)In(C_6H_5) complex crystallizes in the monoclinic system with a space group $P2_1/n$, and the unit cell

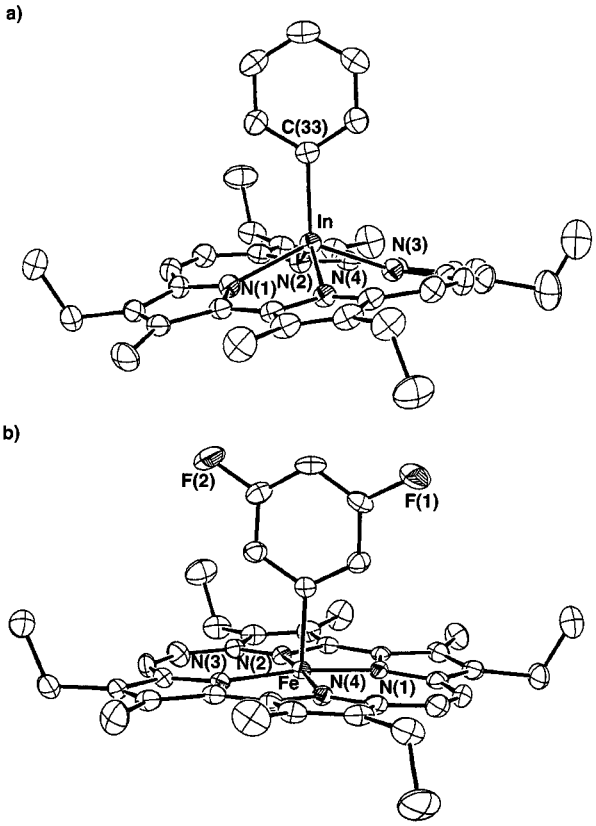

Figure 5. ORTEP views with labeled schemes of the molecular structures of (a) (EtioPc)In(C_6H_5) and (b) (EtioPc)Fe($C_6F_2H_3$).

contains four porphycene units. A view of the molecular structure of (EtioPc)In(C_6H_5) is given in Figure 5a, and selected bond lengths and angles of the coordination polyhedron are summarized in Table 2. The indium atom is pentacoordinated and lies 0.85 Å above the plane of the four porphycenic nitrogen atoms, a distance comparable to the 0.78 Å distance for (TPP)In(CH_3) in the porphyrin series.[50] The In−N bond lengths are almost equal (⟨In−N⟩ = 2.174(3) Å), and, as expected for a rectangular cavity (2.63 × 3.03 $Å^2$), two values are observed for N−In−N angles: 88.3° and 74.5°. The In−C distance is 2.148(3) Å, while that in (TPP)In(CH_3) is 2.13(1) Å.[50] As usually observed for a π ligand, the phenyl group is not in a staggered conformation with respect to the nitrogen atoms.[51] The Φ angle, as introduced by Hoard (see Chart 3),[51] is 22.5°. The weakest steric hindrance is achieved for an angle of 49° with this core geometry. In contrast, an angle of 0° would give the strongest electronic interaction between the p orbitals of the metal and the π orbitals of the macrocycle.[12] The angle observed for this compound is the result of a competition between two effects. The porphycene macrocycle is not planar,

(49) Tabard, A.; Guilard, R.; Kadish, K. M. *Inorg. Chem.* **1986**, *25*, 4277−4285.

(50) Lecomte, C.; Protas, J.; Cocolios, P.; Guilard, R. *Acta Crystallogr., Sect. B: Struct. Sci.* **1980**, *B36*, 2769−2771.

(51) Collins, D. M.; Countryman, R.; Hoard, J. L. *J. Am. Chem. Soc.* **1972**, *94*, 2066−2072.

Chart 3

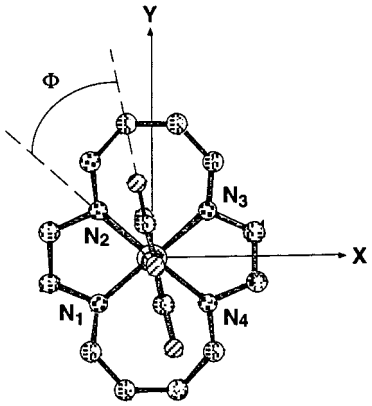

Table 6. Half-Wave Potentials (V vs SCE) for Oxidation and Reduction of (EtioPc)Fe(R) in CH_2Cl_2, 0.2 M TBAP at −50 °C

	$E_{1/2}$ (V vs SCE)				
	oxidation			reduction	
compound	3rd	2nd	1st	1st	2nd
(EtioPc)Fe(C_6H_5)[a]	1.54	1.27	0.44	−1.13	-1.44
(EtioPc)Fe($C_6F_2H_3$)	1.65	1.22	0.59	−1.06	−1.41
(EtioPc)Fe($C_6F_3H_2$)	1.70	1.30	0.60	−0.98	−1.37

[a] Reference 34.

and exhibits a distorted geometry with an undulating effect of the pyrroles. The largest deviations of atoms from the mean porphycene plane are 0.264 and −0.379 Å and the root-mean-square deviation of the 24 fitted atoms from the mean macrocycle plane is 0.183 Å.

Three crystal structures of σ-bonded iron(III)−carbon tetrapyrrolic complexes have been reported in the literature. The first is (TPP)Fe(C_6H_5)[4], where TPP is the dianion of tetraphenylporphyrin while the latter two correspond to (OEC)-Fe^{IV}(C_6H_5) in its neutral form[52] and [(OEC)Fe^{IV}(C_6H_5)]$^{\bullet+}$ where OEC = the dianion of octaethylcorrole.[53] The (EtioPc)Fe-($C_6F_2H_3$) complex crystallized in the monoclinic system $P2_1/n$. Its structure is shown in Figure 5b, and selected bond lengths and angles of the pentacoordination polyhedron are summarized in Table 2. The Fe−N average distance of 1.930(5) Å is shorter than the distance of 1.961(7) Å observed for (TPP)Fe(C_6H_5). As expected for a low-spin iron(III) porphyrin, the iron atom lies close to the mean plane containing the four nitrogen atoms and the Δ4N−metal distance is 0.12 Å. The rectangular core (2.52 × 2.91 Å^2) is contracted in comparison to that of the indium complex and gives two different values for the N−Fe−N angles (81.6° and 97.9°). The ESR data described in the previous section might be explained by this particular geometry. The Fe−C distance of 1.950(4) Å in (EtioPc)Fe($C_6F_2H_3$) is close to that observed in (TPP)Fe(C_6H_5) (1.955(3) Å). The Φ angle, as defined in Chart 3, is equal to 37.2°, and this value is larger than that observed in (EtioPc)In(C_6H_5). This result could be explained by the fact that the iron atom lies close to the macrocyclic plane, thus bringing about a stronger steric interaction between the axial ligand and the macrocycle. The macrocycle of (EtioPc)Fe($C_6F_2H_3$) is rather flat, and the root-mean-square deviation of the 24 fitted atoms from the mean macrocyclic plane is 0.087 Å.

(52) Vogel, E.; Will, S.; Tilling, A. S.; Newman, L.; Lex, J.; Bill, E.; Trautwein, A. X.; Wieghardt, K. *Angew. Chem., Int. Ed. Engl.* **1994**, *33*, 731−735.
(53) Van Caemelbecke, E.; Will, S.; Autret, I.; Adamian, V. A.; Lex, J.; Gisselbrecht, J.-P.; Gross, M.; Vogel, E.; Kadish, K. M. *Inorg. Chem.* **1996**, *35*, 184−192.

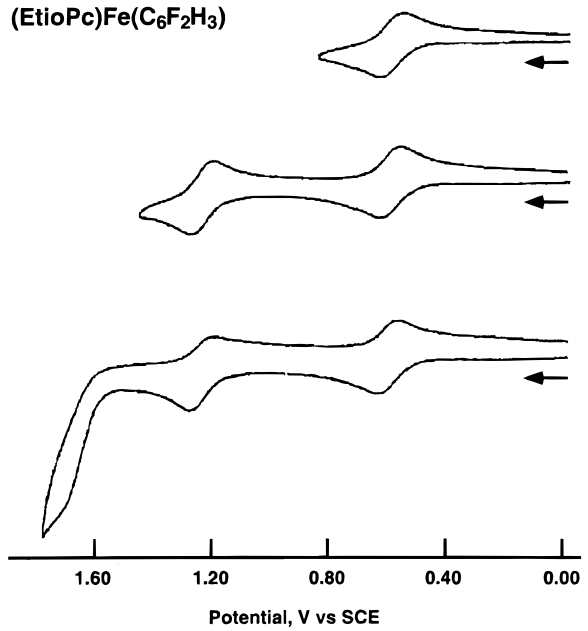

Figure 6. Room-temperature cyclic voltammograms of (EtioPc)Fe-($C_6F_2H_3$) in CH_2Cl_2, 0.1 M TBAP. Scan rate = 0.1 V/s.

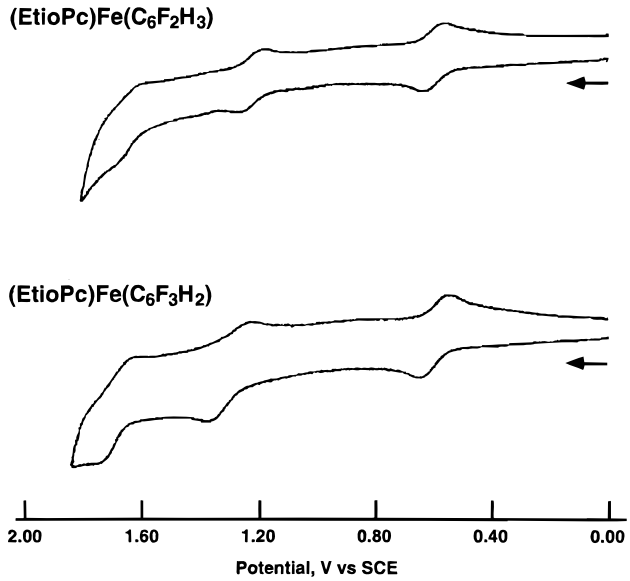

Figure 7. Cyclic voltammograms of (EtioPc)Fe($C_6F_2H_3$) and (EtioPc)-Fe($C_6F_3H_2$) at −50 °C in CH_2Cl_2, 0.1 M TBAP. Scan rate = 0.3 V/s.

Electrochemistry of (EtioPc)Fe(R) in CH_2Cl_2. The electrochemistry of (EtioPc)Fe(C_6H_5) has been reported.[34] The compound undergoes three one-electron oxidations and two one-electron reductions in CH_2Cl_2 at low temperature. The first oxidation involves a metal-centered Fe^{III}/Fe^{IV} reaction while the other four processes are proposed to involve the conjugated π ring system on the basis of both the electrochemistry and UV−visible spectroelectrochemistry of the compound.

Similar oxidative behavior is seen for (EtioPc)Fe(C_6H_5), (EtioPc)Fe($C_6F_2H_3$) and (EtioPc)Fe($C_6F_3H_2$), all of which undergo three oxidations and the formation of Fe(IV) in the first one-electron transfer step (see Table 6). Unfortunately, (EtioPc)Fe(C_6F_4H) was unstable under conditions of the electrochemical experiment and no redox potential could be obtained due to decomposition prior to making the measurement. The first two oxidations of the three stable compounds are reversible in CH_2Cl_2, 0.1 M TBAP, at room temperature and this is shown in Figure 6 for the case of (EtioPc)Fe($C_6F_2H_3$). A third

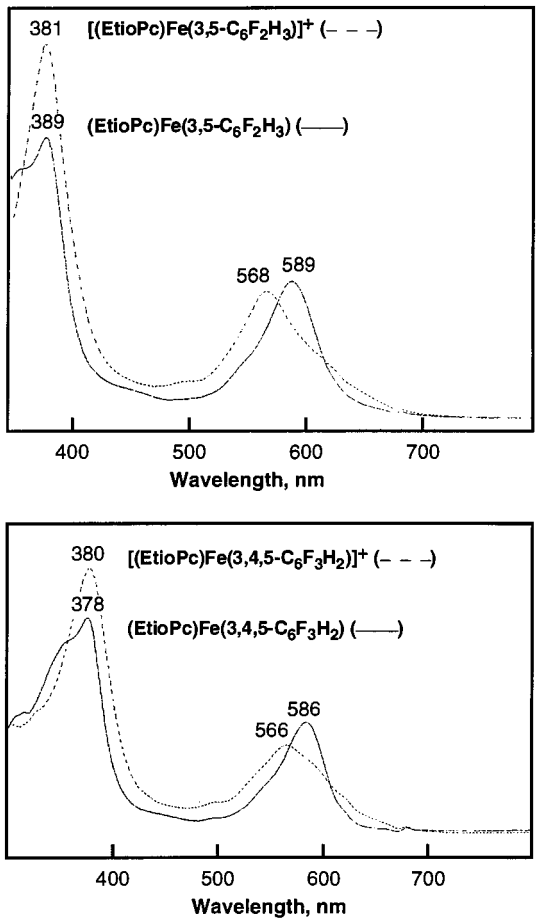

Figure 8. UV−visible spectra before (—) and after (– – –) oxidation of (EtioPc)Fe($C_6F_2H_3$) and (EtioPc)Fe($C_6F_3H_2$) by about 1 equiv of phenoxathiinylium hexachlorantimonate in CH_2Cl_2.

oxidation is located at the edge of the solvent limit at room temperature and is irreversible for (EtioPc)Fe($C_6F_2H_3$) and (EtioPc)Fe($C_6F_3H_2$). However, three reversible oxidations are seen at −50 °C, and this is illustrated in Figure 7. There is no evidence for migration of the axial ligand in the singly or doubly oxidized species on the cyclic voltammetry time scale, but this reaction appears to occur following chemical generation of the singly oxidized species as was previously discussed for the case of (EtioPc)Fe(C_6H_5).[34]

Evidence for the generation of moderately stable [(EtioPc)-Fe^{IV}($C_6F_3H_2$)]$^+$ and [(EtioPc)Fe^{IV}($C_6F_2H_3$)]$^+$ derivatives is given by the UV−visible spectra in Figure 8. The compounds were generated by adding about 1 equiv of phenoxathiinylium hexachloroantimonate to the neutral porphycenes. The Fe(III) and Fe(IV) spectra are quite similar to each other in that each shows a well-defined Soret band and a single visible band which is characteristic of a metalloporphycene with an unoxidized conjugated π ring system.[41] The UV−visible spectra of the oxidized $C_6F_2H_3$ and $C_6F_3H_2$ complexes resemble the published[34] spectrum of [(EtioPc)Fe^{IV}(C_6H_5)]$^+$ and all three singly oxidized complexes have visible bands which fall in the range 566−572 nm. The neutral iron(III) derivatives are blue in CH_2Cl_2, and the color turns purple after addition of the oxidizing agent. However, the σ-bonded iron(IV) porphycenes are only moderately stable in solution and exhibit a change in color from purple to green after about 5−10 min.

The reduction of (EtioPc)Fe($C_6F_2H_3$) and (EtioPc)Fe($C_6F_3H_2$) proceeds via two reversible one-electron transfer steps in CH_2Cl_2, and the $E_{1/2}$ values for each redox process at −50 °C are listed in Table 6. The electrochemical behavior of both porphycenes resembles that of (EtioPc)Fe(C_6H_5), a compound which undergoes only macrocycle-centered electroreductions.[34] The potentials for the first reduction of (EtioPc)Fe($C_6F_2H_3$) and (EtioPc)Fe($C_6F_3H_2$) are shifted anodically by 70 and 150 mV with respect to $E_{1/2}$ values for the first reduction of (EtioPc)-Fe(C_6H_5) and this can be accounted for by the different electron-withdrawing effects of the three axial ligands. The second reduction of the three compounds ranges between $E_{1/2} = -1.37$ and −1.44 V and the absolute potential difference in $E_{1/2}$ between the two reductions varies between 310 and 390 mV depending upon the specific R group (see Table 6). These latter potential differences are consistent with separations of 280 to 410 mV between the two ring-centered reductions of most previously characterized metalloporphycenes containing a variety of different central metal ions.[24,41,54] The key difference between reduction of (EtioPc)Fe(R) and σ-bonded porphyrins such as (OEP)Fe(R), (TPP)Fe(R), or (OETPP)Fe(R) with the same R group is in the site of electron transfer. The porphyrins are all reduced at the metal center to give [(P)Fe^{II}(R)]$^-$ derivatives while the porphycenes are invariably reduced at the macrocycle to give anion radicals represented at [(EtioPc)Fe^{III}(R)]$^-$. The second reduction of the σ-bonded porphyrins occurs at potentials which are shifted negatively by 1.0 or more V from half-wave potentials for the first reduction, and this reaction may or may not involve the metal center. The second reduction of the σ-bonded porphycenes occurs only at the macrocycle, and, as discussed above, gives potentials indicative of this type of reaction.

Acknowledgment. The support of the CNRS and the Robert A. Welch Foundation (K.M.K., E-680) is gratefully acknowledged.

Supporting Information Available: Respectively for (EtioPc)In-(C_6H_5) and (EtioPc)Fe(3,5-$C_6F_2H_3$): ORTEP plots with labeling schemes (Figure SI and SII), complete set of bond distances (Å) and angles (deg) (Tables SIII and SIV), anisotropic displacement parameters (Tables SV and SVI), atomic coordinates and equivalent isotropic displacement parameters (Tables SVII and SVIII), and hydrogen coordinates and isotropic displacement parameters (Tables SIX and SX) (10 pages). Figures SI and SII and Tables SIII−SX have also been deposited with the CCDC and are available on request from the Director of Cambridge Crystallographic Data Center, 12 Union Road, Cambridge CB2 1EZ, (U.K.), on quoting the full journal citation.

IC980610O

(54) Bernard, C.; Gisselbrecht, J. P.; Gross, M.; Vogel, E.; Lausmann, M. *Inorg. Chem.* **1994**, *33*, 2393−2401.